BMC Musculoskeletal Disorders

RESEARCH

Open Access

Mechanisms of pyroptosis in modulating osteoblast function under simulated microgravity

Min Wang[1†], Jindong Xue[1†], Songsong Liu[1], Congncong Xu[1], Zhen Cao[1,2], Haoyang Yu[1], Xiaojuan Nong[1], Kexin Huang[1], Shuling Hu[1], Yong Guo[1,2*] and Biao Han[1,2*]

Abstract

Background Bone mass loss resulting from mechanical unloading in a microgravity environment constitutes a primary impediment to the advancement of space exploration for astronauts. However, the underlying mechanism remains unclear. In this study, we primarily investigated the impact of pyroptosis on osteoblasts under simulated microgravity and its influence on osteoblast functionality.

Methods A rotary cell culture system was employed to establish a simulated microgravity environment. The proliferation of osteoblasts was assessed by cell counting kit-8 (CCK-8) assay. Lactate dehydrogenase (LDH) Release Assay Kit was used to measure cell necrosis. Osteoblast differentiation and mineralization were evaluated using an ALP kit and alizarin red staining. Fluorescence Hoechst/PI double staining and scanning electron microscopy (SEM) were used to detect pyroptosis, and a caspase-1 kit measured caspase-1 activity. The expression of NLRP3, caspase-1, GSDMD, IL-1β, IL-18, OCN, and COL-I was analyzed by qPCR and Western blot. Additionally, ELISA was used to quantify the release of IL-1β and IL-18.

Results The PI fluorescence in osteoblasts exhibited significant enhancement under simulated microgravity conditions, accompanied by increased membrane pore formation, decreased cell proliferation, and elevated LDH release. Moreover, the expression levels of NLRP3, caspase-1, GSDMD, IL-1β, and IL-18 were upregulated while caspase-1 activity was increased. Treatment with MCC950 and VX-765 effectively attenuated pyroptosis levels as well as caspase-1 activity while reducing the expression of NLRP3, GSDMD, IL-1β, and IL-18. Notably, this treatment significantly enhanced the expression of OCN and COL-I.

Conclusion Under simulated microgravity conditions, pyroptosis occurs in osteoblasts and alters their osteogenic differentiation function. Pyroptosis modulates the functionality of osteoblasts and contributes to the mechanical response process, potentially serving as one of the mechanisms underlying mechanical-regulated osteoblast function

†Min Wang and Jindong Xue contributed equally to this work.

*Correspondence:
Yong Guo
guoyong74@126.com
Biao Han
hanbiao@glmc.edu.cn

Full list of author information is available at the end of the article

in a microgravity environment. This finding may offer a novel approach for addressing bone tissue damage and repair under extreme mechanical conditions.

Clinical trial number Not applicable.

Keywords Simulated microgravity, MC3T3-E1cells, Pyroptosis, NLRP3-casepase-1axis

Introduction

Bone mass loss in astronauts, caused by the effects of microgravity, is a major limitation to long-term space missions [1]. The pathological basis of this condition lies in bone tissue cells responding to gravity alterations and developing functional abnormalities [2]. However, the specific mechanisms remain unclear. Studies have demonstrated that the altered mechanical environment is a key factor influencing bone homeostasis [3]. Microgravity, as an extreme mechanical environment, primarily causes bone loss through the continuous mechanical unloading of bone tissue [4]. This condition involves a multifactorial, multi-pathway bone remodeling process, which is characterized by structural changes in bone tissue, functional degradation, and significant impacts on the proliferation, differentiation, and apoptosis of bone-related cells. Additionally, it affects various intracellular genes, proteins, and signaling pathways associated with osteogenesis and resorption, such as ALP, OCN, COL-I, BMPs and RUNX 2 [5]–[8].

Our previous experiments revealed that in the microgravity environment, the inflammatory factor IL-6 in the cell culture medium significantly increased, subjecting osteoblasts to an inflammatory milieu. Pyroptosis, a form of programmed cell death associated with inflammation and immune response, is gaining increasing attention in the field of bone-related diseases [9]. The molecular mechanism of pyroptosis primarily depends on inflammasome-mediated activation of caspase-1, which cleaves gasdermin D (GSDMD), allowing it to bind to the cell membrane, form pores, and induce cell death through swelling, along with the release of mature IL-1β and IL-18 [10, 11]. The NLRP3 inflammasome and the inflammatory cytokines IL-1β and IL-18 play crucial roles in bone homeostasis [12, 13]. Numerous studies have shown that pyroptosis is implicated in the progression of various bone-related diseases and significantly affects osteoblast proliferation and differentiation [14]. One study presented that IL-17 could prompt pyroptosis of osteoblasts further affects bone metabolism [15]. It has been reported that inhibiting caspase-1-mediated cell pyroptosis promotes osteogenic differentiation. Furthermore, in our previous observations of the osteoblast cytoskeleton using a scanning electron microscope, we unexpectedly found that exposure to microgravity induced the appearance of classic "membrane pores" associated with pyroptosis on the osteoblast membrane surface. The aforementioned studies indicate that pyroptosis may be implicated in the growth process of bone tissue cells under inflammatory conditions and exert a significant role. Additionally, pyroptosis is potentially involved as a mechanistic response pathway in bone remodeling triggered by the microgravity environment; however, its precise mechanism warrants further investigation.

The present study aims to investigate the potential effects of cellular pyroptosis on osteoblast proliferation, differentiation, and mineralization under simulated microgravity conditions and to elucidate its underlying mechanisms. Our findings indicate that the functional alterations in osteoblasts under simulated microgravity are mediated by pyroptosis, a process regulated by the NLRP3-caspase 1 axis. We aim to introduce novel perspectives on the mechanical adaptation processes involved in bone remodeling under microgravity or mechanical unloading conditions, thereby providing valuable insights into strategies for mitigating the effects of microgravity and preventing associated bone injuries.

Materials and methods

Cell culture

MC3T3-E1 pre-osteoblast cell line (Mouse Embryonic Osteoblasts Cells, MC3T3-E1Subclone14) was procured from the Chinese Academy of Medical Sciences (Beijing, China) and cultured with the contrast medium which consisted of DMEM, 10% fetal bovine serum, and 1% penicillin/streptomycin solution at 5% CO_2, 37℃. The osteogenic induction medium was composed of the contrast medium supplemented with 10 nM dexamethasone, 50 μg/mL L-ascorbic acid, and 10 mM sodium β-glycerophosphate.

Establishment of microgravity environment

We utilized the NASA-developed Rotary Cell Culture System (RCCS) to simulate microgravity [16–18]. Briefly, cells were inoculated at a density of 1×10^5/mL in a rotary incubator (Synthecon INC, USA), and 5 mL of microcarrier (cytodex 3, GE Healthcare, USA) solution (5 mg/mL) was added. The cells were incubated at a constant speed of 30 rpm/min for 3 days. If air bubbles were detected during incubation, they were immediately removed to prevent fluid shear forces from affecting the cells.

Cell treatment

The experimental groups were organized according to the study design. Each group received the following treatments: the control group (CON) was cultured under normal conditions; the simulated microgravity (SMG) group was cultured in a rotary cell culture system (RCCS); the SMG + MCC950 group was cultured in the RCCS with 10 μM MCC950 in the medium (MCC950 is a selective small molecule inhibitor of NLRP3 inflammasome activation, Proteintech Group, Inc. Wuhan, China); and the SMG + VX765 group was cultured in the RCCS with 10 μM VX-765 (VX-765 is a selective caspase-1 inhibitor, Proteintech Group, Inc. Wuhan, China). Each group was cultured for 3 days for subsequent experiments.

CCK-8 assay

Cells from each group were counted, and the concentration was adjusted to approximately 1×10^4 cells per well before being inoculated into 96-well plates. The plates were incubated at 37℃ in a 5% CO_2 incubator. After 24 h, the medium of each well was replaced by100 μL of 10% CCK-8 solution (Solarbio, China), and the incubation continued at 37℃ for an additional 2 h. And, optical density (OD) values were detected and 490 nm.

ALP activity

Supernatants from each group's cell cultures were collected and centrifuged at 4℃ at 1200 rpm for 10 min. Then, components of the ALP kit (Nanjing Jiancheng Bioengineering Institute, China) were added according to the manufacturer's instructions, and the mixture was gently oscillated. The absorbance of each group was measured using an enzyme-labeled instrument at 520 nm.

Real-time PCR analysis

Cells were collected into centrifuge tubes, and total RNA was extracted using the TRIzol reagent (Invitrogen, USA). cDNA was synthesized via reverse transcription kit (Takara, Japan). RT-PCR was carried out in a total of 20 μL reaction volumes. Samples were analyzed using the $2^{-\Delta\Delta Cq}$ method. The sequences of the primers used are provided in Table 1.

Table 1 Primers sequences in this study

gene	Forward: 5′-3′	Reverse: 5′-3′
NLRP3	GACCAGCCAGAGTGGAATGACA	ACAAATGGAGATGCGGGAGAG
caspase-1	AGAGGATTTCTTAACGGATGCA	TCACAAGACCAGGCATATTCTT
GSDMD	CTAGCTAAGGCTCTGGAGACAA	GATTCTTTTCATCCCAGCAGTC
IL-1β	CTCACAAGCAGAGCACAAGC	CAGTCCAGCCCATACTTTAGG
IL-18	GACTCTTGCGTCAACTTCAAGG	CAGGCTGTCTTTTGTCAACGA
COL-I	CAGTGGCGGTTATGACTT	CTGCGGATGTTCTCAATCT
OCN	AGTCTGACAAAGCCTTCA	AAGCAGGGTTAAGCTCACA
ALP	AAGGAGGCAGGATTGAC	ATCAGCAGTAACCACAGTC
GAPDH	CAGCAACTCCCACTCTTC	TGTAGCCGTATTCATTGTC

Western blotting

Cells from each group were collected, and protein was extracted using RIPA lysate and quantified using the BCA method. Following quantification, 30 μg of protein was combined with 4× sample buffer and boiled in water for 10 min. The sample was then loaded into an electrophoresis system containing a prepared 15% separating gel and a 5% stacking gel for electrophoresis. After electrophoresis, the gel was cut and transferred to a PVDF membrane. Following membrane transfer, the PVDF membrane was incubated with 5% fat-free milk for 2 h at room temperature. The membrane was then incubated overnight at 4 °C with primary antibodies (abcam, USA), including NLRP3 (1:2000 dilution), caspase-1 (1:2000 dilution), GSDMD (1:1000 dilution), IL-1β (1:2000 dilution), IL-18 (1:2000 dilution), OCN (1:500 dilution), COL-I (1:5000 dilution), and β-actin (1:50000 dilution). The membrane was subsequently washed five times with TBST and then incubated with a goat anti-rabbit secondary antibody (1:5000 dilution) at room temperature for 2 h, followed by five additional washes with TBST. The ECL chemiluminescent solution was applied, and the images were developed using a gel imaging system. The results were then analyzed using ImageJ software.

Alizarin red staining

The MC3T3-E1 cells from the CON group and the SMG group were separately digested from the microcarriers, after which cells were seeded in 6-well plates at a density of 2×10^4 cells/cm². Upon reaching 80–95% confluence, the complete osteogenic induction differentiation medium was added to the plates, and the medium was replaced by half every 48 h. The cells were cultured for 14 days in 6-well plates. Subsequently, the culture medium was removed, and the cells were washed twice with PBS. They were then fixed using an adequate amount of Olympus Brightfield (OB, Solarbio, China) fixative for 15 min and washed three times with PBS, with each wash lasting 3 min. Subsequently, an appropriate amount of alizarin red staining solution was added dropwise, and the cells were stained for 30 min at room temperature in the dark, followed by three washes with double-distilled water. Finally, the stained cells were washed and examined under a microscope.

Scanning electron microscopy (SEM)

Cell groups were placed in 1.5 mL centrifuge tubes. The cells were then fixed in 2.5% glutaraldehyde for 2 h at

room temperature and subsequently stored overnight at 4 °C. The fixed cells were washed with PBS buffer, post-fixed in 1% osmium tetroxide (OsO4) for 1.5 h, and dehydrated using a series of ethanol concentrations: 50%, 70%, 80%, 90%, and 100%. The samples were dried at the critical point, mounted on short columns, sputtered with a thin platinum (Pt) film, and subsequently observed under SEM.

Hoechst/PI double staining

Osteoblasts from each group were re-inoculated into 24-well plates at a density of 3×10^5 cells per well and incubated at 37 °C in a cell culture incubator for 48 h. After incubation, the cells were washed twice with PBS. Following this, 0.8 mL of cell staining buffer was added, along with 5 μL of both Hoechst and PI staining solutions (Apex Bio, USA). The mixture was thoroughly mixed and incubated at 4 °C for 30 min to complete the staining process. Finally, the cells were washed with PBS and examined under a microscope.

Lactate dehydrogenase (LDH) assay

Cell supernatants were collected from each group, and lactate dehydrogenase (LDH, Beyotime, Haimen, China) levels were measured using an LDH kit to assess cell membrane integrity. To determine the maximum LDH release, cells were treated with the LDH release reagent for 60 min before the assay. The LDH release rate was calculated using the following formula: Release Rate (%) = (OD490nm experimental group - OD490nm negative control group) / (OD490nm positive control group - OD490nm negative control group) × 100%.

Caspase-1 activity assay

The activation of caspase-1 in osteoblasts was assessed using an activity assay kit (Beyotime, China). This kit relies on the enzymatic reaction where caspase-1 catalyzes the cleavage of Ac-YVAD-pNA (Acetyl-Tyr-Val-Ala-Asp) to release yellow pNA (p-nitroaniline). Following the manufacturer's instructions, approximately 1×10^6 extracted cells were lysed in 200 μL of protein lysis buffer to achieve a final protein concentration of 1 ~ 3 mg/mL. The cell lysates were then centrifuged at 16,000 × g for 15 min at 4 °C. Subsequently, 50 μL of the supernatant was incubated with 0.2 mM Ac-YVAD-pNA in the reaction buffer at 37 °C for 2 h. Absorbance was measured at 405 nm using a spectrophotometer.

Enzyme-linked immunosorbent assay (ELISA)

The secretion of interleukin-1 beta (IL-1β, Beyotime, Haimen, China) and interleukin-18 (IL-18, Beyotime, Haimen, China) in the cell culture supernatants of each group was measured using ELISA kits, following the manufacturer's instructions. The cell supernatant was centrifuged at 3000 rpm for 10 min. Subsequently, 50 μL of standard products with varying concentrations were added to the designated wells for standards, while 10 μL of the sample to be tested was added to the sample wells, followed by 40 μL of sample diluent. Next, except for the blank wells, 100 μL of horseradish peroxidase (HRP)-labeled detection antibody was added to each well of both the standard and sample wells. The reaction wells were then sealed with a sealing film and incubated in a 37 °C water bath for 60 min. Following incubation, 50 μL of substrate A and 50 μL of substrate B were added to each well, and the mixture was further incubated in the dark at 37 °C for 15 min. Finally, 50 μL of termination solution was added to each well to halt the enzymatic reaction, and the optical density (OD) values of each well were measured at a wavelength of 450 nm.

Flow cytometry

Cell apoptosis was analyzed using the Annexin V-FITC/PI staining method. When the cell fusion of each group reaches 80 ~ 90%, digest the cells using trypsin without EDTA and collect them. Wash the cells twice with pre-cooled PBS and adjust the cell concentration to 2×10^5. Add 500 μL of binding buffer and gently pipette to resuspend the cells. Then, add 5 μL of Annexin V-FITC followed by 5 μL of PI, and incubate at room temperature in the dark for 15 min. Analyze the samples by flow cytometry.

Statistical analysis

All data are presented as the means ± standard deviation (SD). The statistical analysis was conducted by GraphPad Prism. *P*-values < 0.05 were considered statistically significant. All data were obtained from experiments performed in triplicate.

Result

Proliferation, differentiation, apoptosis and mineralization of osteoblasts were inhibited under simulated microgravity

To investigate the functional alterations in osteoblasts before and after exposure to microgravity, we employed CCK-8 assays, quantitative real-time PCR (qRT-PCR), Western blot analysis, flow cytometry, and alizarin red staining to evaluate osteoblast proliferation, differentiation, apoptosis, and mineralization, respectively. As shown in Fig. 1A, the CCK-8 assay demonstrated a significant reduction in the proliferation rate of MC3T3-E1 osteoblasts in the SMG group compared to the CON group. The ALP activity assay indicated a significant reduction in ALP levels in the simulated microgravity group compared to the control group, moreover, the gene and protein expression levels of osteoblast differentiation markers, such as Col-I, and OCN, were significantly

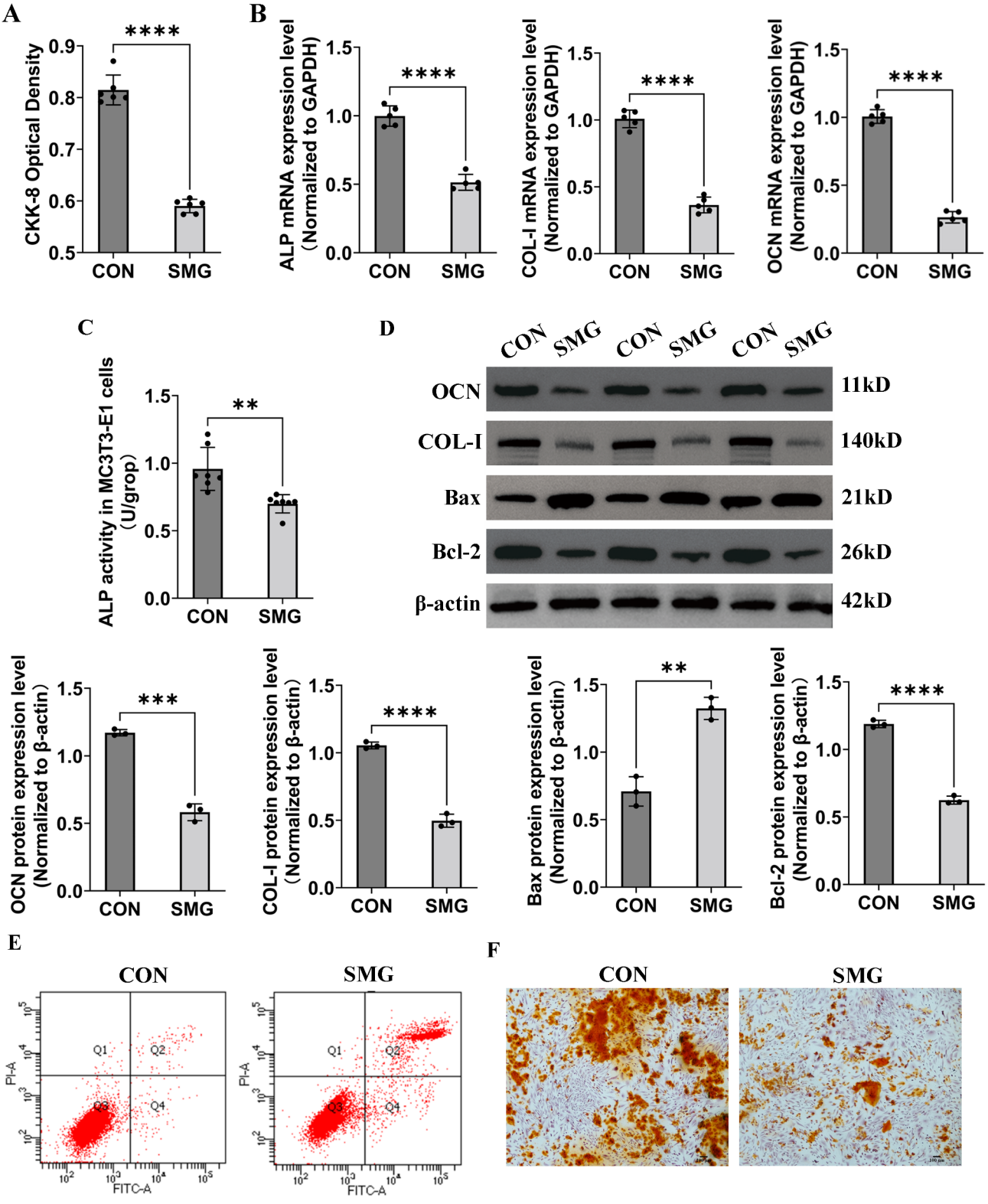

Fig. 1 Altered osteoblast function is observed under simulated microgravity condition. **A**. The CCK-8 assay was employed to evaluate the proliferative activity of osteoblasts ($n=6$). **B**. The mRNA expression levels of ALP, OCN, and COL-I were assessed using qRT-PCR ($n=5$). **C**. ALP activity in MC3T3-E1 cells ($n=7$). **D**. The protein expression levels of OCN, COL-I, Bax and Bcl-2 were assessed using western blot ($n=3$). **E**. Cell apoptosis was assessed using flow cytometry analysis ($n=3$). **F**. Alizarin red staining was utilized to assess the mineralization of osteoblasts ($n=3$, bar = 100 μm). ** $p<0.01$, *** $p<0.001$, **** $p< 0.0001$

downregulated (Fig. 1B-D). The flow cytometry analysis revealed a significantly higher incidence of early apoptosis in osteoblasts under simulated microgravity conditions compared to the control group (Fig. 1F). Additionally, the expression levels of apoptosis-related proteins BAX and Bcl-2 were examined. The findings indicated that simulated microgravity led to a significant upregulation of Bax expression and a concurrent significant downregulation of Bcl-2 expression. The alizarin red staining results demonstrated a significant inhibition of osteoblast mineralization under simulated microgravity conditions compared to the control group (Fig. 1G). These findings suggest that simulated microgravity conditions significantly inhibit the proliferation, differentiation, and mineralization of osteoblasts while promoting apoptosis.

Simulated microgravity promotes pyroptosis in osteoblasts

To investigate the specific mechanisms underlying the functional alterations of osteoblasts in a simulated microgravity environment, we initially conducted scanning electron microscopy (SEM) analyses to examine the membrane integrity of osteoblasts. As shown in Fig. 2A, SEM images show distinct morphological features of osteoblast pyrolysis under simulated microgravity conditions. Visible cell membrane rupture and pore formation indicating impaired cell membrane integrity suggests the characterization of pyroptosis. The lactate dehydrogenase (LDH) assay was utilized to quantify the levels of pyroptosis, revealing a significant elevation in LDH release from osteoblasts exposed to simulated microgravity in comparison to the control group (Fig. 2B). Caspase-1 activity serves as an indicator of the pyroptotic response in osteoblasts, and the findings demonstrated that simulated microgravity elicited a significantly elevated response compared to the control group (Fig. 2C). The results from western blot assays demonstrated significant increases in the expression levels of pyroptosis-related proteins in osteoblasts exposed to SMG compared to the CON group, such as NLRP3, caspase-1, GSDMD, IL-1β, and IL-18 (Fig. 2D). These findings demonstrate that pyroptosis occurs in osteoblasts under simulated microgravity conditions, and this process is associated with the regulation of the NLRP3-caspase-1 axis.

Pyroptosis of osteoblasts is regulated through NLRP3-casepase1 axis in simulated microgravity

To investigate whether the pyroptosis of osteoblasts under simulated microgravity is regulated via the NLRP3-caspase-1 axis, osteoblasts were pretreated with MCC950, a selective inhibitor of NLRP3, and VX765, a specific inhibitor of caspase-1. The results demonstrated that pretreatment with MCC950 or VX765 significantly decreased LDH release and caspase-1 activity in comparison to the SMG group (Fig. 3A, B). Furthermore, SEM analysis revealed that, in comparison to the SMG group, the pretreatment with MCC950 or VX765 resulted in a reduction in both the size and number of membrane pores on the cell surface (Fig. 3C). This suggests that the administration of MCC950 or VX765 can effectively inhibit pyroptosis in osteoblasts under the simulated microgravity condition. Moreover, the alterations in the gene and protein expression levels of NLRP3, caspase-1, GSDMD, IL-1β, and IL-18 were consistent with the aforementioned findings (Fig. 3D, E). These results indicate that pyroptosis induced by simulated microgravity is mediated via the NLRP3-caspase-1 pathway.

The functional alterations in osteoblasts under simulated microgravity are attributed to pyroptosis

Finally, we investigated whether the altered function of osteoblasts under simulated microgravity was

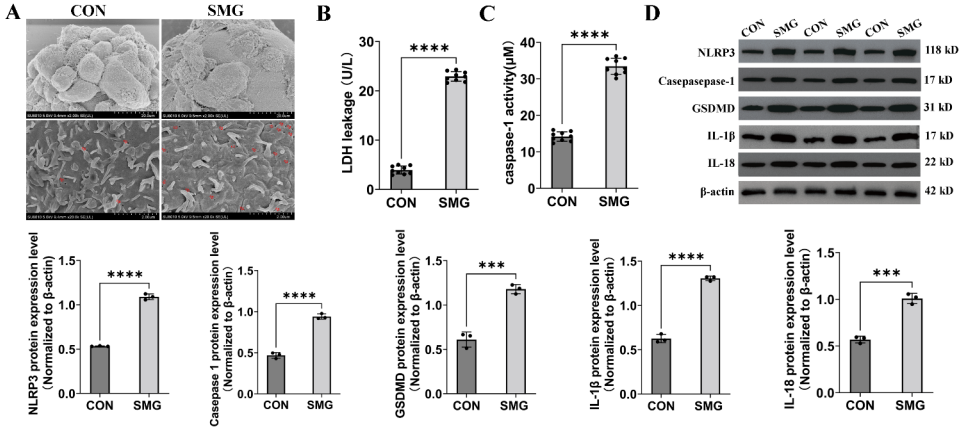

Fig. 2 Detection of pyroptosis in osteoblasts under simulated microgravity conditions. **A**. The morphological characteristics of osteoblasts were observed via SEM before and after exposure to simulated microgravity 72 h (2000 ×, bar = 20 μm, 20000 ×, bar = 2 μm, red arrows represent cell membrane rupture and pore formation). **B** and **C**. LDH assay and casepase-1 activity in MC3T3-E1cells ($n = 9$). **D**. The protein expression levels of NLRP3, casepase-1, GSDMD, IL-1β and IL-18 were assessed using western blot ($n = 3$). *** $p<0.001$, **** $p< 0.0001$

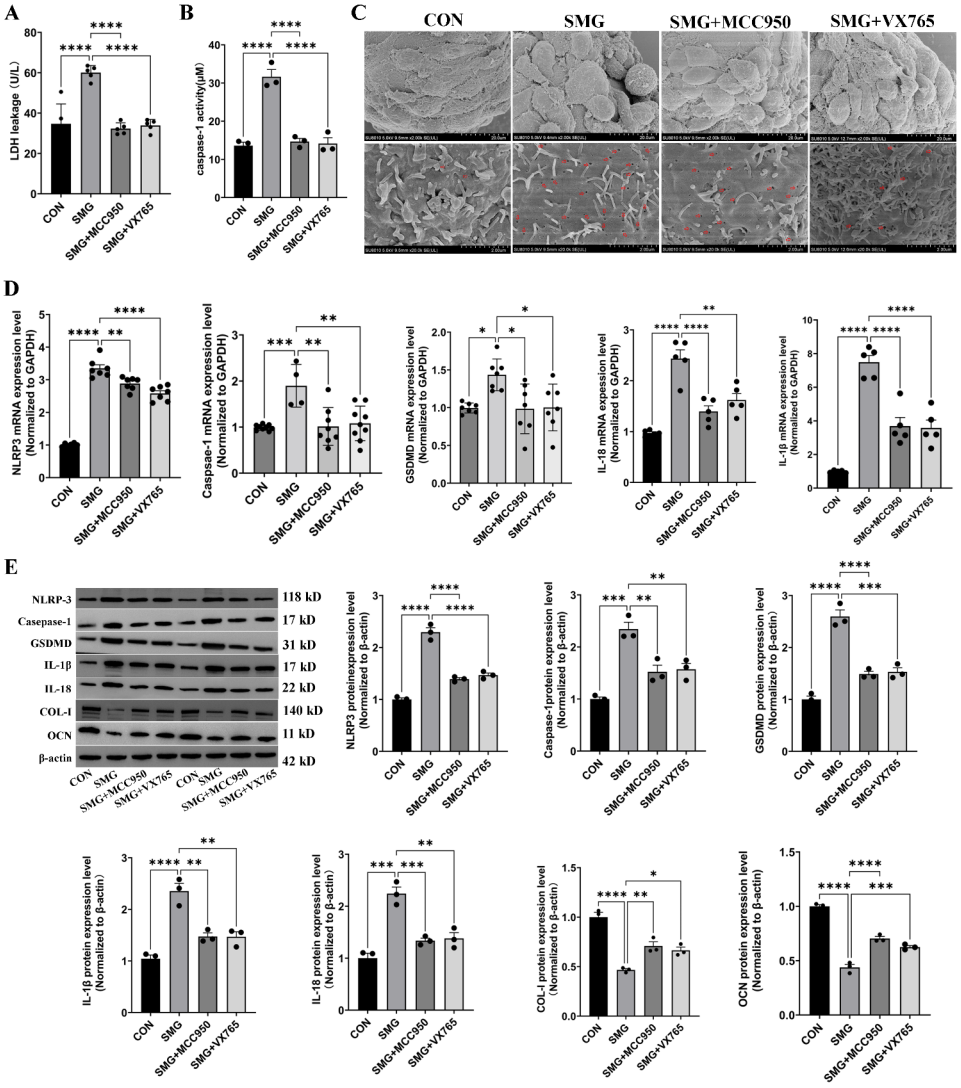

Fig. 3 The pyroptosis of osteoblasts under simulated microgravity is modulated by the NLRP3-caspase-1 axis. **A** and **B**. LDH assay and casepase-1 activity in MC3T3-E1cells ($n=7$). **C**. The morphological characteristics of osteoblasts were observed via SEM before and after exposure to simulated microgravity 72 h (2000 ×, bar = 20 μm, 20000 ×, bar = 2 μm, red arrows represent cell membrane rupture and pore formation). **D**. The mRNA expression levels of NLRP3, casepase-1, GSDMD, IL-1β and IL-18 were assessed using qRT-PCR ($n=7$). **E**. The protein expression levels of NLRP3, casepase-1, GSDMD, IL-1β, IL-18, COL-I and OCN were assessed using western blot ($n=3$). * $p<0.05$,** $p<0.01$, *** $p<0.001$, **** $p< 0.0001$

attributable to pyroptosis in osteoblasts. As shown in Fig. 4, CCK-8 assay result suggests that pre-treated with MCC950 or VX765 significantly enhanced the proliferation of MC3T3-E1 osteoblasts exposed to SMG conditions compared to SMG group (Fig. 4A). Furthermore, ALP activity was significantly enhanced in osteoblasts treated with MCC950 or VX765. Additionally, the gene and protein expression levels of osteoblast differentiation markers, including Col-I and OCN, were markedly upregulated following the introduction of NLRP3 and caspase-1 inhibitors (Figs. 3E and 4B and C). Hoechst/PI double staining revealed that osteoblasts in the SMG group displayed an increased number of cells with weak red and strong blue fluorescence characteristics. However, this effect was reversed upon the addition of MCC950 or VX765(Fig. 4D). The osteoblast mineralization, as assessed by Alizarin red staining, indicates that the inhibition of NLRP3 or caspase-1 expression significantly enhances the mineralization of osteoblasts.

Discussion

Osteoblasts play a crucial role in bone formation and remodeling, and their activity is highly sensitive to mechanical and gravitational signals [19]. The microgravity conditions experienced in space significantly affect bone reconstruction, resulting in decreased bone density and impaired bone regeneration [20]. Previous studies have demonstrated that cell proliferation and

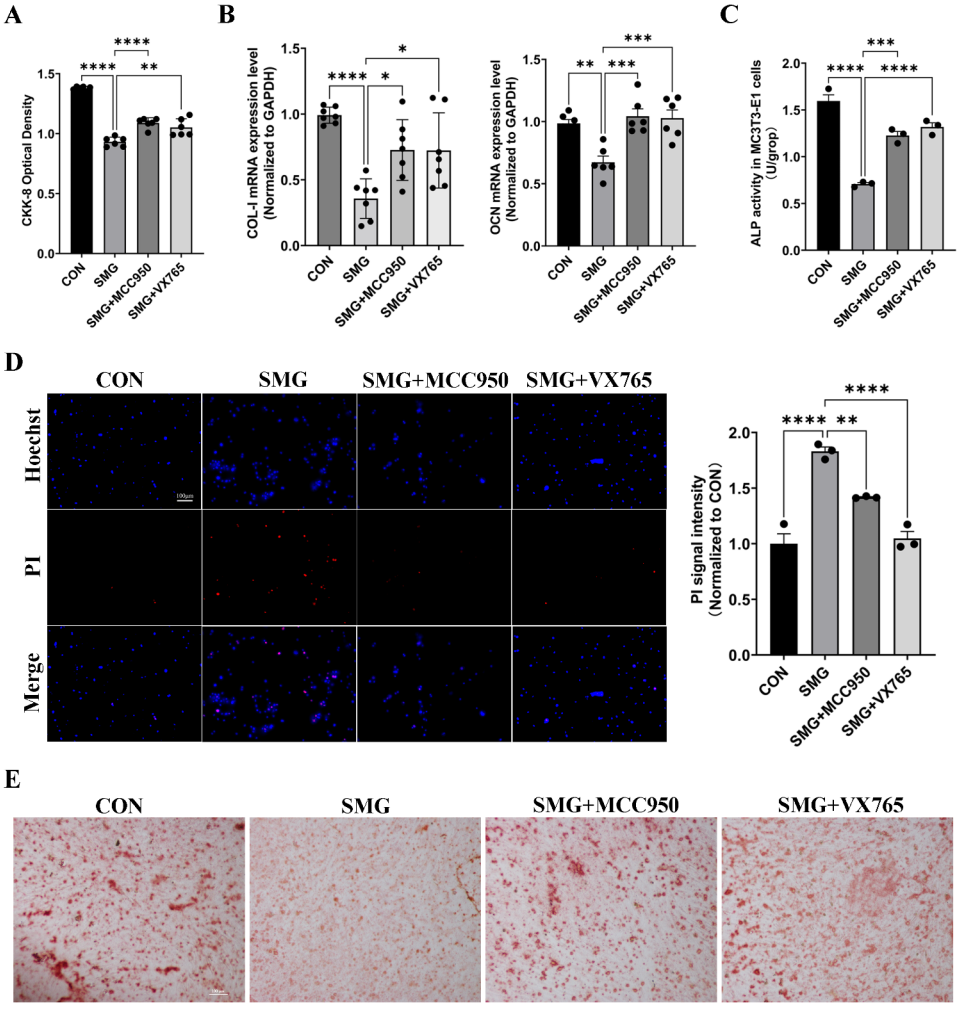

Fig. 4 The proliferation, differentiation, apoptosis, and mineralization of osteoblasts are regulated by the NLRP3-caspase-1 axis. **A**. The CCK-8 assay was employed to evaluate the proliferative activity of osteoblasts ($n=6$). **B**. The mRNA expression levels of ALP, OCN, and COL-I were assessed using qRT-PCR ($n=7$). **C**. ALP activity in MC3T3-E1 cells ($n=3$). **D**. Cell apoptosis was assessed using Hoechst/PI double staining ($n=3$). **E**. Alizarin red staining was utilized to assess the mineralization of osteoblasts ($n=3$, bar = 100 μm). * $p<0.05$,** $p<0.01$, *** $p<0.001$, **** $p< 0.0001$

differentiation are notably inhibited under simulated microgravity conditions. However, the precise mechanism by which simulated microgravity modulates osteoblast proliferation and differentiation remains unclear. In this study, we discovered that simulated microgravity can inhibit osteoblast proliferation and differentiation by activating the pyroptosis pathway.

Pyroptosis is an inflammatory caspase mediated process of necrotic cell death, and its importance is becoming increasingly prominent [21]. The typical feature of cell pyroptosis is the formation of membrane pores [22]. SEM observations revealed numerous membrane pores on the surface of cells in the SMG group, consistent with prior findings. Hoechst 33,342 is a cell penetrant dye that binds to nuclear DNA, while propidium iodide (PI) is widely used for detecting cell necrosis or pyroptosis due to its inability to penetrate normal living cells. Following SMG treatment, PI fluorescence intensity was significantly higher in the SMG group than in the control group. LDH release and caspase-1 activity can evaluate pyroptosis levels [23]. The SEM and PI results, combined with LDH release and caspase-1 activity results, indicates significant pyroptosis in osteoblasts under SMG conditions. Elevated LDH release and caspase-1 activity suggested a shift toward pyroptosis, potentially impairing osteoblast function and contributing to bone loss. The activation of caspase-1 implies that the inflammatory pathway is involved in the cellular response to microgravity. The canonical pathway of pyroptosis activates NLRP3 signaling to form inflammasomes and recruit caspase-1 [24]. Subsequently, activated caspase-1 cleaves GSDMD, IL-1β, and IL-18 [25, 26]. qPCR and Western blot analysis indicated significant increases in the expression and activation of inflammasome components NLRP3, caspase-1, GSDMD, IL-1β, and IL-18 under SMG. Furthermore, treatment with competitive inhibitors MCC950 and

VX765 targeting NLRP3 and caspase-1 led to reduced expression of NLRP3, caspase-1, GSDMD, IL-1β, and IL-18, reinforcing the pathway's role in cell pyroptosis under microgravity. This suggests that pyroptosis in osteoblasts is linked to the NLRP3/caspase-1 signaling pathway.

In this study, we investigated the role of pytoptosis in the proliferation and differentiation of osteoblasts. Research shows that cell activity significantly affects the maintenance of normal osteogenic function [26]. SMG markedly inhibited cell proliferation, which improved upon the introduction of pytoptosis inhibitors. This finding underscores the impact of pyroptosis on osteoblast activity. The osteogenic marker patterns typically include ALP, OCN, COL-I, all of which are associated with bone formation and widely used to indicate osteogenic differentiation [27, 28]. Osteogenic differentiation and mineralization were evaluated by ALP activity and alizarin red staining [29]. ALP, a marker for osteogenic differentiation, exhibited reduced activity under simulated microgravity but increased following pyroptosis inhibition. Additionally, mineralized nodule staining demonstrated that pyroptosis inhibits osteogenic differentiation. The expression and activation levels of COL-I and OCN, critical markers for osteogenic differentiation, were also significantly reduced under simulated microgravity but improved with pyroptosis inhibition. These results suggest that targeting pyroptosis inhibition could be a promising strategy for mitigating bone loss.

Benefits and limitations

This study elucidates the mechanisms of bone loss in microgravity, which is critical for advancing space exploration. By identifying pyroptosis as a pivotal factor influencing osteoblast function, this research introduces a novel direction for investigation. The findings may facilitate the development of therapies targeting bone damage both in space and on Earth. Furthermore, the emphasis on pyroptosis expands the scope of inquiry within bone biology. However, it is important to note that the sample size and diversity are restricted, focusing primarily on osteoblasts under simulated microgravity conditions, which might not fully replicate real space environments. Additionally, the rotary cell culture system represents an artificial model requiring further validation for in vivo applications. Lastly, while the study examines short-term effects, the long-term implications remain to be explored.

Conclusion

Under simulated microgravity conditions, osteoblasts induce pyroptosis via the NLRP3/caspase-1 pathway. After inhibiting pyroptosis, the proliferation of osteoblasts and the level of osteogenic differentiation increase. However, its specific mechanism requires further investigation. These findings enhance our understanding of bone loss mechanisms during prolonged space exploration and mechanical unloading conditions.

Supplementary Information

The online version contains supplementary material available at https://doi.org/10.1186/s12891-025-08629-5.

Supplementary Material 1

Supplementary Material 2

Acknowledgements
Not applicable.

Author contributions
WM was responsible for overseeing the implementation of cell experiments, XJD oversaw the execution of protein experiments, LSS and XCC performed statistical analysis, CZ conducted bioinformatics analysis, YHY and NXJ were in charge of data collation and mapping, HKX and HSL contributed to certain experimental procedures, while GY and HB were involved in experimental design and paper writing.

Funding
The present study was supported by the National Natural Science Foundation of China (grant no. 12202113), Guangxi Natural Science Foundation (grant no. AD22080037, 2020GXNSFBA238006) and the National Natural Science Foundation of China (grant no. 12462030, 32071309). These agencies were not involved in the design of the study; collection, analysis, and interpretation of data; and manuscript writing.

Data availability
The data and materials are available from the corresponding author on request.

Declarations

Ethics approval and consent to participate
Not applicable.

Consent for publication
Not applicable.

Competing interests
The authors declare no competing interests.

Author details
[1]College of Intelligent Medicine and Biotechnology, Guilin Medical University, Guilin 541199, China
[2]Key Laboratory of Medical Biotechnology and Translational Medicine, Education Department of Guangxi Zhuang Autonomous Region, Guilin 541199, China

Received: 26 December 2024 / Accepted: 7 April 2025
Published online: 24 April 2025

References

1. Man J, Graham T, Squires-Donelly G, Laslett AL. The effects of microgravity on bone structure and function. Npj Microgravity. 2022;8(1):1–15. https://doi.org/10.1038/s41526-022-00194-8.
2. Wubshet NH, Cai G, Chen SJ, et al. Cellular mechanotransduction of human osteoblasts in microgravity. Npj Microgravity. 2024;10(1):1–12. https://doi.org/10.1038/s41526-024-00386-4.
3. Carvajal-Agudelo JD, McNeil A, Franz-Odendaal TA. Effects of simulated microgravity and vibration on osteoblast and osteoclast activity in cultured

zebrafish scales. Life Sci Space Res. 2023;38:39–45. https://doi.org/10.1016/j.lssr.2023.05.002.
4. Juhl OJ, Buettmann EG, Friedman MA, DeNapoli RC, Hoppock GA, Donahue HJ. Update on the effects of microgravity on the musculoskeletal system. Npj Microgravity. 2021;7(1):1–15. https://doi.org/10.1038/s41526-021-00158-4.
5. Liu P, Tu J, Wang W, et al. Effects of mechanical stress stimulation on function and expression mechanism of osteoblasts. Front Bioeng Biotechnol. 2022;10. https://doi.org/10.3389/fbioe.2022.830722.
6. Rutkovskiy A, Stensløkken KO, Vaage IJ. Osteoblast differentiation at a glance. Med Sci Monit Basic Res. 2016;22:95–106. https://doi.org/10.12659/MSMBR.901142.
7. Pardo SJ, Patel MJ, Sykes MC, et al. Simulated microgravity using the random positioning machine inhibits differentiation and alters gene expression profiles of 2T3 preosteoblasts. Am J Physiology-Cell Physiol Published Online June. 2005;1. https://doi.org/10.1152/ajpcell.00222.2004.
8. Wang D, Cai J, Zeng Z, et al. The interactions between mTOR and NF-κB: A novel mechanism mediating mechanical stretch-stimulated osteoblast differentiation. J Cell Physiol. 2021;236(6):4592–603. https://doi.org/10.1002/jcp.30184.
9. Li X, Ji L, Men X, et al. Pyroptosis in bone loss. Apoptosis. 2023;28(3):293–312. https://doi.org/10.1007/s10495-022-01807-z.
10. Ding J, Wang K, Liu W, et al. Pore-forming activity and structural autoinhibition of the gasdermin family. Nature. 2016;535(7610):111–6. https://doi.org/10.1038/nature18590.
11. Li Z, Ji S, Jiang ML, Xu Y, Zhang CJ. The regulation and modification of GSDMD signaling in diseases. Front Immunol. 2022;13. https://doi.org/10.3389/fimmu.2022.893912.
12. Chen Y, Yang Q, Lv C, et al. NLRP3 regulates alveolar bone loss in ligature-induced periodontitis by promoting osteoclastic differentiation. Cell Prolif. 2021;54(2):e12973. https://doi.org/10.1111/cpr.12973.
13. Rocha FRG, Delitto AE, de Souza JAC, González-Maldonado LA, Wallet SM, Rossa Junior C. Relevance of Caspase-1 and Nlrp3 inflammasome on inflammatory bone resorption in A murine model of periodontitis. Sci Rep. 2020;10(1):7823. https://doi.org/10.1038/s41598-020-64685-y.
14. Murakami T, Nakaminami Y, Takahata Y, Hata K, Nishimura R. Activation and function of NLRP3 inflammasome in bone and Joint-Related diseases. Int J Mol Sci. 2022;23(10):5365. https://doi.org/10.3390/ijms23105365.
15. Lei L, Sun J, Han J, Jiang X, Wang Z, Chen L. Interleukin-17 induces pyroptosis in osteoblasts through the NLRP3 inflammasome pathway in vitro. Int Immunopharmacol. 2021;96:107781. https://doi.org/10.1016/j.intimp.2021.107781.
16. Sambandam Y, Townsend MT, Pierce JJ et al. Microgravity control of autophagy modulates osteoclastogenesis. *Bone*. 2014;61:125– 31. https://doi.org/10.1016/j.bone.2014.01.004
17. Pellegrini M, Di Siena S, Claps G et al. Microgravity promotes differentiation and meiotic entry of postnatal mouse male germ cells. *PLoS One*. 2010;5(2):e9064. https://doi.org/10.1371/journal.pone.0009064
18. Luo H, Zhu B, Zhang Y, et al. Tissue-engineered nerve constructs under a microgravity system for peripheral nerve regeneration. Tissue Eng Part A. 2015;21(1–2):267–76. https://doi.org/10.1089/ten.TEA.2013.0565.
19. Xiao W, Wang Y, Pacios S, Li S, Graves DT. Cellular and molecular aspects of bone remodeling. Front Oral Biol. 2016;18:9–16. https://doi.org/10.1159/000351895.
20. Xu L, Zhang X, Li G, et al. Inhibition of SIRT1 by miR-138-5p provides a mechanism for inhibiting osteoblast proliferation and promoting apoptosis under simulated microgravity. Life Sci Space Res (Amst). 2023;36:59–69. https://doi.org/10.1016/j.lssr.2022.08.001.
21. Yang L, Liu J, Shan Q, Geng G, Shao P. High glucose inhibits proliferation and differentiation of osteoblast in alveolar bone by inducing pyroptosis. Biochem Biophys Res Commun. 2020;522(2):471–8. https://doi.org/10.1016/j.bbrc.2019.11.080.
22. Chen X, He WT, Hu L, et al. Pyroptosis is driven by non-selective gasdermin-D pore and its morphology is different from MLKL channel-mediated necroptosis. Cell Res. 2016;26(9):1007–20. https://doi.org/10.1038/cr.2016.100.
23. Wang X, Fan L, Yin H, et al. Protective effect of aster Tataricus extract on NLRP3-mediated pyroptosis of bladder urothelial cells. J Cell Mol Med. 2020;24(22):13336–45. https://doi.org/10.1111/jcmm.15952.
24. Yao Y, Chen S, Cao M, et al. Antigen-specific CD8 + T cell feedback activates NLRP3 inflammasome in antigen-presenting cells through Perforin. Nat Commun. 2017;8(1):15402. https://doi.org/10.1038/ncomms15402.
25. Shi J, Zhao Y, Wang K, et al. Cleavage of GSDMD by inflammatory caspases determines pyroptotic cell death. Nature. 2015;526(7575):660–5. https://doi.org/10.1038/nature15514.
26. Dai ZQ, Wang R, Ling SK, Wan YM, Li YH. Simulated microgravity inhibits the proliferation and osteogenesis of rat bone marrow mesenchymal stem cells. Cell Prolif. 2007;40(5):671. https://doi.org/10.1111/j.1365-2184.2007.00461.x.
27. Li W, Zhang S, Liu J, Liu Y, Liang Q. Vitamin K2 stimulates MC3T3–E1 osteoblast differentiation and mineralization through autophagy induction. Mol Med Rep. 2019;19(5):3676–84. https://doi.org/10.3892/mmr.2019.10040.
28. Sun LJ, Li C, Wen XH, et al. Icariin stimulates hFOB 1.19 osteoblast proliferation and differentiation via OPG/RANKL mediated by the Estrogen receptor. Curr Pharm Biotechnol. 2021;22(1):168–75. https://doi.org/10.2174/1389201021666200123102550.
29. Ariffin SHZ, Wahab RMA, Razak MA, et al. Evaluation of in vitro osteoblast and osteoclast differentiation from stem cell: a systematic review of morphological assays and staining techniques. PeerJ. 2024;12:e17790. https://doi.org/10.7717/peerj.17790.

Publisher's note